Colloid Polym Sci 274:399–409 (1996)

ORIGINAL CONTRIBUTION

K.M. McGrath

Polymerisation of liquid crystalline phases in binary surfactant/water systems.

Part 2. ω-undecenyltrimethylammonium bromide

Received: 9 March 1995
Accepted: 26 October 1995

K.M. McGrath[1]
Department of Applied Mathematics
Research School of Physical Sciences
and Engineering
The Australian National University
Canberra ACT 0200, Australia

[1]*Present address*:
Dr. K.M. McGrath (✉)
Department of Physics
Princeton University
P.O. Box 708
Princeton, New Jersey 08544, USA

Abstract The self-assembly behaviour of the polymerisable surfactant ω-undecenyltrimethylammonium bromide (ω-UTAB) both before and after polymerisation has been investigated. In addition polymerisation of the liquid crystalline phases formed by this surfactant in aqueous solution has been studied. Introduction of the carbon-carbon double bond at the end of the hydrocarbon chain increases the rigidity of the paraffinic chains such that the Krafft curve is shifted to higher temperatures compared with that of dodecyltrimethylammonium bromide, a non-polymerisable analogue. Both the polymerised and non-polymerised forms have been observed to have the same phase progression, with the polymer being more soluble in water such that the liquid crystalline phases formed at high surfactant concentration are accessible at room temperature. Polymerisation of the liquid crystalline phases of ω-UTAB indicate that polymerisation proceeds to approximately 40% (in comparison with 80% in a non-aggregated form) and that the original monomeric matrix is undisturbed upon partial polymerisation.

Key words Polymerisation – surfactant self-assembly – liquid crystals – ω-undecenyltrimethylammonium bromide

Introduction

In the first paper of this series [1] the phase behaviour and polymerisation of two quaternary ammonium surfactants containing the allyl polymerisable moiety within the head group of the surfactant were discussed. In this paper, results are reported for the surfactant ω-undecenyltrimethylammonium bromide (ω-UTAB, $CH_2=CH-(CH_2)_9-N^+(CH_3)_4Br^-$) where the position of the allyl polymerisable moiety is shifted from the head group to the end of the hydrocarbon chain. This surfactant, therefore, has an identical head group to dodecyltrimethylammonium bromide (DTAB, $CH_3-(CH_2)_{11}-N^+(CH_3)_3Br^-$) differing only in the nature of the hydrocarbon tail [2–7]. Hence their phase behaviour is directly comparable. The presence of the allyl polymerisable moiety has two consequences. Firstly due to the increased hydrophilicity of the group (as compared with a methyl group) the hydrophobicity of the paraffinic tail is decreased and secondly the length of the chain is effectively reduced (the presence of the double bond has been shown to be equivalent to reducing the chain length by approximately one CH_2 group [8]). These effects should therefore manifest themselves in the subsequent self-assembly of the surfactant molecules.

It was observed from the self-assembly of allyldodecyldimethylammonium bromide (ADAB, $CH_3-(CH_2)_{11}-N^+(CH_3)_2(CH_2-CH=CH_2)Br^-$) [1] that the presence of the allyl moiety in the head group of the surfactant, not

only, increased the solubility of the surfactant but also reduced the stability of the liquid crystalline phases to increases in temperature. The inclusion of the allyl group at the tail of the paraffinic chain should not introduce such a perturbation. Although, the hydrophilic nature of the allyl moiety will lead to an increased stability of the individual surfactant molecules in aqueous solution (i.e. the onset of surfactant aggregation should be shifted to higher surfactant concentrations). Once the surfactant molecules have aggregated the subsequent phase progression should not be dominated by the presence of the polymerisable moiety (since this will on average be confined to the hydrophobic core) unlike the ADAB/water self-assembly [1]. That is, the ω-UTAB phase diagram should more closely resemble that of DTAB [2–7] rather than ADAB [1].

In addition to the change in position of the allyl moiety affecting the surfactant's self-assembly, a change in the rate and extent/ease of polymerisation both before and after self-assembly should be observed. By placing the allyl group at the end of the hydrocarbon chain both the electrostatic and steric interactions experienced when the allyl group was incorporated in the head group [1] will be significantly reduced. Therefore polymerisations, at least in the non-self-assembled form should be facilitated. Moving the site at which polymerisation occurs away from the interfacial area also increases the likelihood of retention of the underlying surfactant geometry. That is, when polymerisation is initiated at a location isolated from the region where the effects of several competing interactions are concentrated (e.g. electrostatic forces, interfacial tension, hydration forces, molecular packing constraints and film curvature and rigidity) the likelihood of any perturbations to these interactions caused by the onset of polymerisation is markedly reduced as compared with when polymerisation occurs within this region. The increased mobility experienced by the polymerisable moiety in this position may though, disrupt the orientation of the carbon-carbon double bonds (crucial for polymerisation) such that, any free radical formed may be lost before it is able to propagate the polymerisation.

Hence, by altering the position of the polymerisable group both the self-assembly and subsequent polymerisation of the surfactant monomers will be affected.

Experimental

ω-UTAB was prepared from ω-undecenol (99% pure, purchased from Aldrich Chemical Co., Inc.) using a standard method for bromination of an alcohol with a secondary functional group [9]. The final precipitated product was obtained by bubbling trimethylamine gas through a solution of ω-undecenyl bromide in ethyl acetate at room temperature for several hours. Elemental Analysis: Calculated for $C_{14}H_{30}NBr$:C 57.53%; H 10.34%; N 4.79%; Br 27.34%. Found C 57.6%; H 10.25%; N 4.57%; Br 27.58%. Decomposition temperature 192 °C. NMR Analysis: Proton $(CH_2)_5$–$(CH_2)_2$–N 1.27 δ; CH_2–CH_2–$CH=C$ 1.36 δ; CH_2–CH_2–N 1.75 δ; CH_2–$CH=C$ 2.04 δ; $(CH_3)_3$–N 3.47 δ; CH_2–N 3.63 δ; $CH_2=C$ doublet of doublets centred at 4.96 δ; $CH=C$ 5.80 δ. Carbon 13 CH_2–CH_2–N 22.97 δ; CH_2–CH_2–$CH=C$ 25.92 δ; $(CH_2)_5$–$(CH_2)_2$–$CH=C$ 29.04 δ; CH_2–$CH=C$ 33.51 δ; $(CH_3)_3$–N 53.10 δ; CH_2–N 66.57 δ; $=CH_2$ 113.95 δ; $=CH$ 138.83 δ. FTIR Analysis: C=C stretch 1638.0 cm^{-1}; H–C= stretch 3017.2 cm^{-1}.

All experimental techniques were as described in the first paper of this series [1].

Results

Critical micelle concentration

The surface tension measurements of ω-UTAB for concentrations between 4×10^{-3} and 0.15 M obtained by the du Noüy tensiometry method at 25 °C are shown in Fig. 1. The break in the experimental data points gives an indication of the concentration at which surfactant aggregation is initiated (i.e., the critical micelle concentration (cmc)). The pre-micellisation data points were fitted with a second order polynomial (correlation coefficient = 1.000) [10, 11] and the cmc was calculated to be 5.38×10^{-2} M. The

Fig. 1 Surface tension/concentration curve for the ω-UTAB/water system, measured by the du Noüy ring method at 25 °C. Errors are indicated by the size of the data points

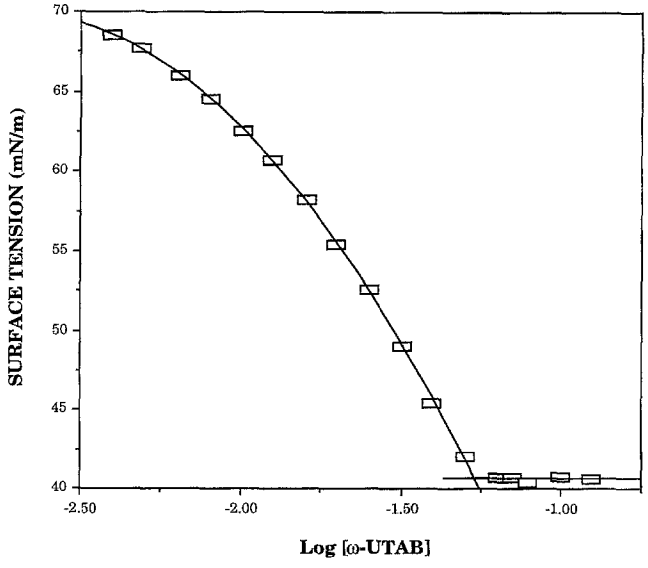

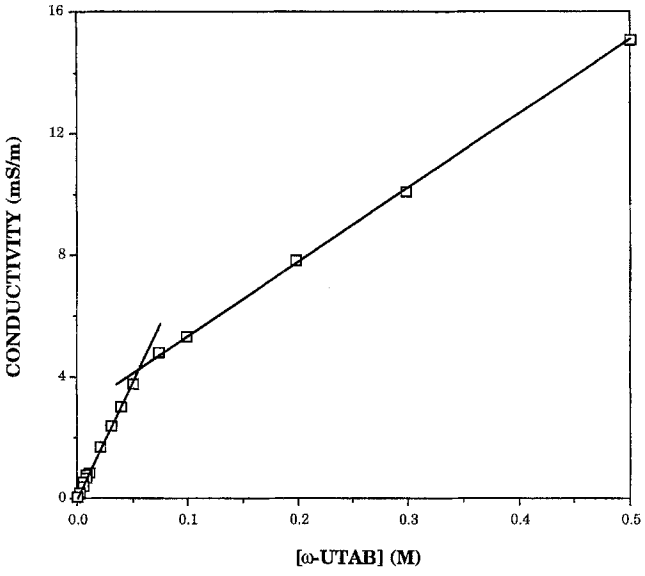

Fig. 2 Electrical conductivity of ω-UTAB in water at 25 °C. Errors are indicated by the size of the data points

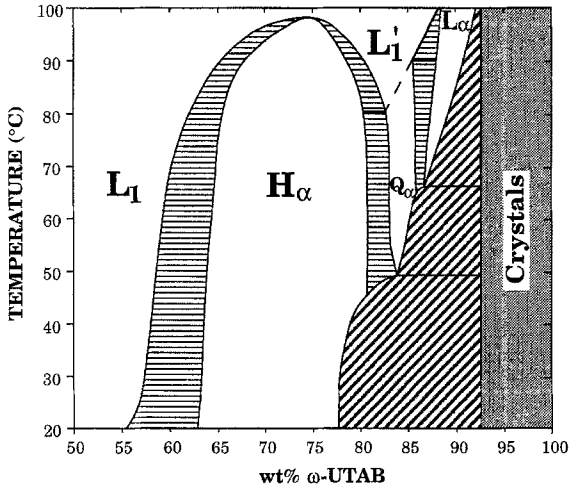

Fig. 3 Schematic partial binary phase diagram of the ω-UTAB/water system. L_1: micellar solution, H_α: hexagonal phase, Q_α: bicontinuous cubic phase (type Q^{230}, Ia3d or Gyroid IPMS), L_1': isotropic fluid, L_α: lamellar phase, and crystals: hydrated ω-UTAB crystals. Horizontally shaded areas indicate regions where two liquid crystalline phases coexist (indicating tie lines), diagonally shaded areas indicate regions where a liquid crystalline phase coexists with hydrated crystals of ω-UTAB

excess concentration of ω-UTAB at the interface was determined to be $3.5 \pm 0.1 \times 10^{-3}$ mol·cm^{-2} and the area per polar head group is equal to 47 ± 1 Å [1].

Figure 2 shows the corresponding electrical conductivity measurements. Again, the initiation of surfactant aggregation is evidenced by the break in the electrical conductivity/ω-UTAB concentration curve. The cmc was found to occur at 5.71×10^{-2} M ω-UTAB using linear fits for the data points both before and after the onset of surfactant aggregation. The percentage dissociation (β) of the bromide counterions calculated from the ratio of the slopes of these linear fits is 32.9%. β may also be determined using a monodisperse mass-action model [1, 6, 12–14]. Tabor and Underwood [15] have measured the average aggregation number (n) of the ω-UTAB micelles, at the cmc, to be 31 (from light scattering measurements). Using this value of n, β is calculated to be 33.3%. Therefore, the average percentage dissociation of the bromide counterions upon micellisation is approximately 33%.

The cmc of ω-UTAB (5.3×10^{-2} M) as determined by Tabor and Underwood [15] is comparable to those values obtained here.

Monomeric self-assembly

For the binary ω-UTAB/water system, three liquid crystalline phases are formed at temperatures between 20° and 100 °C. A hexagonal phase (H_α) forms at 20 °C between 63.2 and 77.4% by weight. A cubic phase (Q_α) forms at 83.7 wt% ω-UTAB but is not observed until temperatures in excess of 49.5 °C are achieved. The final liquid crystalline phase observed, the lamellar phase (L_α), forms at 66.5 °C and 86.6% by weight of ω-UTAB. The partial phase diagram for this system, as determined here, is shown schematically in Fig. 3.

Results from concentration gradients performed at various temperatures indicate that no phases other than the hexagonal, cubic and lamellar are formed in the temperature range of 20° to 100 °C, and that hydrated ω-UTAB crystals are present at all temperatures.

Figure 4 shows a typical optical texture observed through crossed polarising filters for samples within the ω-UTAB hexagonal region of the phase diagram. This texture is an example of the "fan texture" commonly observed for hexagonal phases [16, 17] where the primary axes of the hexagonal cylinders lie parallel to the glass slide [18]. This photograph shows the presence of line disclinations of order $s = +1/2$ which may be paired such that, the two disclinations coincide (i.e., two sets of brushes met at a single point) or are influenced by one another but displaced in space. The disclinations may also remain unpaired. The brushes of the line disclinations lie at an angle of between 5° and 10°, indicating that the hexagonal phase is non-uniaxial [19]. The brushes rotate in the same sense as the polariser and analyser which indicates a positive disclination order. Edge dislocation in the underlying surfactant geometry are also apparent by the sharp black boundaries between the fans.

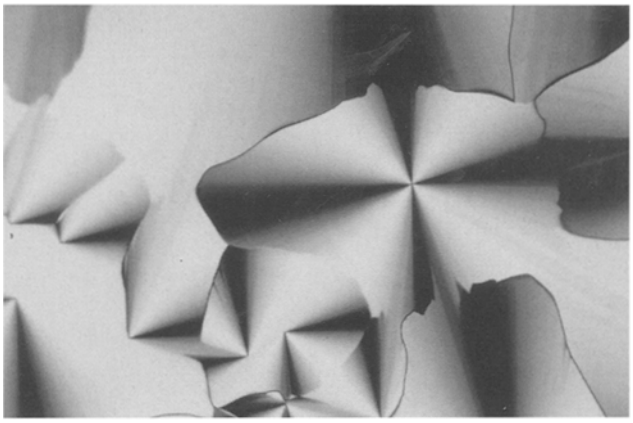

Fig. 4 Fan texture of the ω-UTAB hexagonal phase (crossed polarising filters, magnification 240). The cylinders lie parallel to the glass slide and the brushes correspond to line disclination of strength $s = +1/2$. The brushes lie at an angle of between 5° to 10° to the polariser and analyser. Edge dislocations between individual fans are indicated by sharp dark lines, (60.0 wt% ω-UTAB sample at 25 °C)

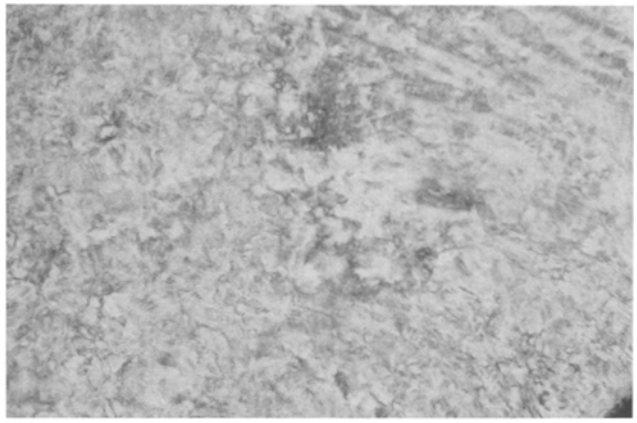

Fig. 5 Mosaic texture of the ω-UTAB lamellar phase (crossed polarising filters, magnification 240). The layers comprising the phase lie parallel to the glass slide, (87.2 wt% ω-UTAB sample at 83.8 °C)

As the temperature increases the hexagonal phase melts at 98 °C and the transition between the two isotropic fluid phases (L_1 and L_1') becomes continuous.

The stability of the cubic phase (Q_α) formed in the ω-UTAB/water system is restricted in both temperature and composition forming only above temperatures of 49.5 °C and melting at 90.8 °C.

The optical texture observed for a sample in the ω-UTAB lamellar phase when viewed through crossed polarising filters is shown in Fig. 5. The texture yields little information on the underlying surfactant geometry, in that few clear features are apparent, though it is possible to discern some maltese crosses within the general sandstone background. This texture is normally termed "mosaic" [16, 20–22] and is in general formed when the sample adopts a homeotropic orientation. Due to the insolubility of the surfactant at high concentrations the lamellar, like the cubic phase is not observed until the temperature has been raised, but the phase remains stable up to 100 °C. The lamellar phase has also been observed to have a large temperature hysteresis. On decreasing the temperature from the pure lamellar phase the transition temperature is found to be lowered by approximately 40 °C as compared to when the temperature is increased. Therefore, in this temperature range a supercooled lamellar state exists which is metastable. Both the cubic and hexagonal phases are not observed with decreasing temperature from the lamellar phase.

Assignments of the regions in the phase diagram were established by determination of the structures with small-angle x-ray scattering (SAXS). Diffraction patterns were obtained for powdered bulk samples in the micellar, hexagonal, cubic and lamellar phases and were comprised of Debye–Scherrer rings which were produced by all domains in the irradiated volume.

Samples within the L_1 isotropic fluid phase produced diffraction patterns at small- and wide-angles comprised of one diffuse ring only [23].

The diffraction pattern of the bulk hexagonal phase of ω-UTAB at small-angles consists of five sharp rings in the ratios of 1: $\sqrt{3}$: $\sqrt{4}$: $\sqrt{7}$: $\sqrt{9}$ as expected for parallel cylinders packed in a two-dimensional array (Table 1). The wide-angle scattering showed one diffuse ring located at $2\pi/4.5 = 1.4$ Å^{-1} indicating a liquid-like state for the paraffinic chains [23], this was true of the cubic and lamellar phases also.

The ω-UTAB cubic phase is characterised by five sharp rings at small-angles with Q values in the ratios of $\sqrt{6}$: $\sqrt{8}$: $\sqrt{14}$: $\sqrt{16}$: $\sqrt{20}$. These ratios being characteristic of one cubic phase only, the Q^{230} (Ia3d) which is assumed here to be bicontinuous as has been shown in other systems [3, 24–27]. This phase has been observed experimentally to be either of type I or of type II but due to the placement of the phase in the self-assembly progression of ω-UTAB it is most likely to be of type I. This phase has also been ascribed to the Gyroid infinite periodic minimal surface (IPMS) having genus = 5 [28–33].

Samples in the lamellar liquid crystalline phase of ω-UTAB produced diffraction patterns at small-angles comprised of two sharp rings only, in the ratio of 1:2 as expected for parallel planer bilayers [23].

From the locations of the Bragg peaks the unit cell dimensions can be calculated assuming that the symmetry of the aggregates is higher than the symmetry of the array and that there is complete segregation of the paraffin and polar regions [23]. The structural parameters for the

Table 1 Structural parameters for the surfactant aggregates formed in the ω-UTAB/water system at $T = 27\,^{\circ}C$

ω-UTAB % (w/w)	Phase	Observed Q ($\AA^{-1}$)	Unit cell length (a) (Å)	Volume fraction Φ	Surfactant aggregate thickness (d_s) (Å)	Water thickness (d_w) (Å)	Mean area per polar head (A) ($\AA^2$)	hkl
39.9	L_1	0.171	–	0.37	–	–	–	–
54.9	L_1	0.188	–	0.52	–	–	–	–
57.0	L_1 +	0.190	–	0.54	–	–	–	–
63.2	H_α	0.201	36.1	0.60	29.4	6.6	58.8	$10\bar{1}0$
		0.347						$11\bar{2}0$
		0.401						$20\bar{2}0$
		0.534						$21\bar{3}0$
		0.604						$30\bar{3}0$
65.1	H_α	0.203	35.7	0.62	29.6	6.1	58.5	$10\bar{1}0$
		0.350						$11\bar{2}0$
		0.408						$20\bar{2}0$
		0.456						$21\bar{3}0$
70.0	H_α	0.208	34.8	0.67	30.0	4.8	57.6	$10\bar{1}0$
		0.360						$11\bar{2}0$
		0.415						$20\bar{2}0$
		0.463						$21\bar{3}0$
		0.551						$30\bar{3}0$
75.2	H_α	0.213	34.0	0.73	30.5	3.5	56.8	$10\bar{1}0$
		0.370						$11\bar{2}0$
		0.425						$20\bar{2}0$
		0.478						$21\bar{3}0$
		0.563						$30\bar{3}0$
83.0[a]	Q_α (Ia3d)	0.216	71.28	0.83	–	–	–	211
		0.249						220
		0.330						321
		0.352						400
		0.395						420
84.9[a]	Q_α (Ia3d)	0.221	69.65	0.85	–	–	–	211
		0.254						220
		0.337						321
		0.360						400
		0.405						420
88.5[b]	L_α	0.236	26.6	0.88	23.3	3.3	38.3	001
		0.476						002
90.0[b]	L_α	0.239	26.3	0.89	23.4	2.9	38.1	001
		0.486						002

[a] temperature = 70 °C
[b] temperature = 90 °C

self-assembled states observed in the ω-UTAB/water system obtained using these assumptions are given in Table 1. The specific volume of ω-UTAB was approximated by calculating the specific volume of the paraffinic chains and from measurements of the specific volume of the trimethylammonium head group [23, 34–41]. All equations were calculated for $T = 27\,^{\circ}C$ unless stated otherwise.

Polymeric ω-UTAB

Polymerisation of the monomeric form of ω-UTAB in chloroform (in which the surfactant does not self-assemble) using both photochemical (direct decomposition of the monomer) and thermal (via decomposition of added α, α'-Azobis(isobutyronitrile) (AIBN, $(CH_3)_2C(CN)\,N{=}N(CN)\,C(CH_3)_2$)) initiation has been investigated. Results indicate that polymers obtained from either method were similar.

By studying the self-assembly of polymeric ω-UTAB it is possible to determine if there are overlapping regions between the polymeric and monomeric phase behaviour. Any overlap which does occur increases the likelihood (i.e., there is an increased probability) that polymerisation of the monomeric liquid crystalline phases within this overlap region will lead to a retention of the underlying surfactant geometry upon polymerisation.

Polymeric ω-UTAB was prepared by thermal initiation (10 mol% to surfactant) in a 0.25 M chloroform solution. The reaction mixture was maintained at 60 °C for 7 days after which the polymerisation had preceded to approximately 80%. Increasing the reaction time did not increase the extent of polymerisation significantly. The so formed polymer had a molecular weight cut-off of approximately 8000 (i.e., $\sim$ 30 monomer units per polymer chain as determined by dialysis). Pure polymer was obtained by removal of the monomer and oligomer units using Sephadex G-15, a size exclusion gel filtration packing material, having a molecular weight cut-off of 1500.

NMR Analysis (as analysed for head-to-tail polymerisation): Proton $(C\underline{H}_2)_5$–$(CH_2)_2$–N 1.26 δ; $C\underline{H}_2$–$(CH_2)_7$–N 1.41 δ; $C\underline{H}_2$–CH_2–N 1.74 δ; $C\underline{H}$–$(CH_2)_3$ 2.01 δ; $(C\underline{H}_2)_2$–CH–CH_2 2.15 δ; $C\underline{H}_2$–$(CH_2)_8$–N 2.63 δ; $(C\underline{H}_3)_3$–N 3.45 δ; $C\underline{H}_2$–N 3.58 δ. Carbon 13 $\underline{C}H_2$–CH_2–N 22.92 δ; $(\underline{C}H_2)_2$–CH–CH_2 26.08 δ; $\underline{C}H_2$–$(CH_2)_7$–N 26.15 δ; $\underline{C}H_2$–$(CH_2)_8$–N 28.31 δ; $(\underline{C}H_2)_5$–$(CH_2)_2$–N 29.23 δ; $(\underline{C}H_3)_3$–N 52.77 δ; $\underline{C}H$–$(CH_2)_3$ 54.92 δ; $\underline{C}H_2$–N 66.15 δ (compare with NMR analysis of monomer experimental section).

Unfortunately, polymeric ω-UTAB is extremely hydroscopic and a full phase diagram was not obtained. Concentration gradients only were performed in the temperature range 20° to 100 °C where new samples were used for each new temperature.

Comparison with the phase behaviour of monomeric ω-UTAB shows that the solubility of the surfactant has been significantly increased upon polymerisation allowing access to both cubic and lamellar phases at 20 °C (i.e., the overall stability of these phases has been increased). Due to the polymers hygroscopic nature no pure hydrated polymer crystals were observed, coexisting with the lamellar liquid crystalline phase only. From a 25 °C concentration gradient the observed phase formation is a micellar (L_1), hexagonal (H_α), cubic (Q_α, assigned due to the extremely high viscosity of the phase as compared with the micellar isotropic phase) and lamellar (L_α) phases, the later coexisting with hydrated polymeric ω-UTAB crystals. As the temperature is increased the lamellar phase exists as a pure phase above 30 °C. At higher temperatures the polymeric phase behaviour mirrors that of the monomeric self-assembly. At 70 °C the cubic phase begins to melt forming a second fluid isotropic phase (L_1', Fig. 6) and is completely melted by 75 °C (which is approximately 15 °C lower than was observed in the monomeric phase progression). The L_1, H_α, L_1' and L_α phases persist up to 95 °C where the hexagonal phase melts and there is a continuous transition between the two isotropic fluid phases. Hence, the monomeric and polymeric forms of ω-UTAB have been observed to self-assemble in water with a similar phase progression.

It should be noted that although the monomeric ω-UTAB/water system is a binary (or pseudo ternary system, where the counterions comprise the third phase) the polymeric ω-UTAB/water system is a multicomponent system due to the polydispersity of the polymer units. This will also be the case for polymerisation of lyotropic liquid crystalline phases due to the polymerisation reaction in the two being identical.

Fig. 6 View of a 70 °C concentration gradient for the polymeric ω-UTAB/water system under crossed polarising light. The cubic phase now coexisting with an isotropic fluid (L_1'), (magnification 240)

Due to the significant similarity of the monomeric and polymeric ω-UTAB/water phase progressions and the high conversion of monomer to polymer during isotropic polymerisation in chloroform the probability that the underlying surfactant geometry in the liquid crystalline phase will be retained upon polymerisation is increased.

Polymerisation of liquid crystalline phases

Unfortunately, due to the inaccessibility of the cubic and lamellar phases at room temperature these phases were not able to be polymerised. For a phase to be polymerisable by the two methods employed here it must be accessible at low temperatures, since for thermally activated samples, equilibration must take place at low temperatures to ensure that polymerisation does not commence prior to obtaining a fully equilibrated state and the photochemical reaction chamber is run at 30 °C only.

The hexagonal and micellar regions of the ω-UTAB/water system were therefore the only regions studied. Polymerisation samples were prepared, by the freeze–thaw–pump method, for 5 (dilute micellar phase), 40 (concentrated micellar phase) and 70 (hexagonal phase) wt% ω-UTAB. The surfactant was not observed to self-initiate during equilibration.

Table 2 shows the percentage conversions for the three regions of the ω-UTAB/water system activated by thermal

Table 2 Percentage conversions for the three regions of the ω-UTAB/water phase diagram polymerised either thermally or photochemically

Type of initiation	Time (days)	Dilute micellar phase	Concentrated micellar phase	Hexagonal phase
Thermal initiation	0.17	26.6	24.5	–
	0.25	30.7	23.6	39.6
	0.5	44.7	24.4	–
	0.71	23.2	–	–
	0.75	30.7	29.1	34.0
	1.0	–	28.4	35.0
	1.33	22.1	–	–
	2.0	37.5	34.8	43.7
	3.0	35.1	40.9	–
	4.0	47.2	37.4	46.9
	6.0	31.7	37.4	46.6
	7.0	–	34.6	–
	8.0	40.7	41.2	38.2
	10.0	42.8	36.7	46.8
	12.0	40.0	38.5	35.3
	14.0	–	35.7	41.0
	15.0	23.1	34.1	–
	20.0	34.7	–	–
Photochemical initiation	0.17	38.4	32.2	34.2
	0.5	42.8	17.1	22.0
	0.75	40.6	19.4	30.1
	1.0	23.1	17.3	38.3
	2.0	37.7	25.7	27.5
	3.0	29.6	20.8	13.3
	4.0	30.4	24.2	23.1
	6.0	26.8	16.7	19.6
	8.0	35.9	25.9	27.5
	10.0	18.4	15.3	33.9
	12.0	25.1	19.3	28.7
	14.0	33.6	14.9	31.1

initiation of added AIBN (10 mol% to surfactant) at 60 °C or photochemically. Note that an error of approximately $\pm$ 5% can be expected in these values due to inaccuracies in the measured integration values.

Whether initiated thermally or photochemically similar results were obtained for all samples. The major discrepancies occurring for the concentrated micellar solutions where the extent of polymerisation via photochemical initiation was considerably lower than that observed for thermal initiation, which also appeared to have an activation time of approximately 2 days before the extent of polymerisation plateaus out. This was not observed for any other region. The reason for this difference in the two methods of initiation for this region of the phase diagram is unknown.

The calculated mean and median for the polymerisations in the different regions are given in Table 3 which indicate that polymerisation via thermal initiation is on average more successful. It should be noted that the extent of polymerisation is reduced significantly as compared with polymerisation of ω-UTAB in an isotropic state (which was found to polymerise to approximately 80%). Hence, the extent of polymerisation is reduced upon surfactant self-assembly.

To determine the affect that polymerisation has had on the underlying surfactant geometry, samples in each region were exposed for 5 days at 60 °C (using 10 mol% AIBN as initiator). Both micellar solutions were found to remain optically isotropic upon polymerisation and while the molecular weight of the polymer was found to be less than 8000 (i.e., less than 30 monomer units) which is comparable to the molecular weight of the monomeric micellar aggregates (at least in the dilute micellar phase region, as determined by Tabor and Underwood [15]) this does not ensure intra-micellar polymerisation (i.e., formation of a "polymerised micelle" see the Discussion section).

The partially polymerised hexagonal phase was also found to produce optical textures similar to those observed for a pure monomeric hexagonal phase (see Fig. 7). Here, edge dislocations and line disclination of order $s = +1/2$ are still observed and the brushes of the fan remain splayed due to variations in the curvature of groups of cylinders. The hexagonal phase begins to melt at approximately 80 °C entering a two phase region with an

Colloid & Polymer Science, Vol. 274, No. 5 (1996)

Table 3 Statistics of the extent of polymerisation for the three ω-UTAB liquid crystalline phases

		Low weight percent micellar solution	High weight percent micellar solution	Hexagonal phase
Thermal initiation	median	34.7	34.8	41.0
	mean	34.0	33.4	40.8
	standard deviation	7.9	5.7	4.6
Photochemical initiation	median	32.0	19.4	28.1
	mean	31.9	20.7	27.4
	standard deviation	7.2	5.0	6.7

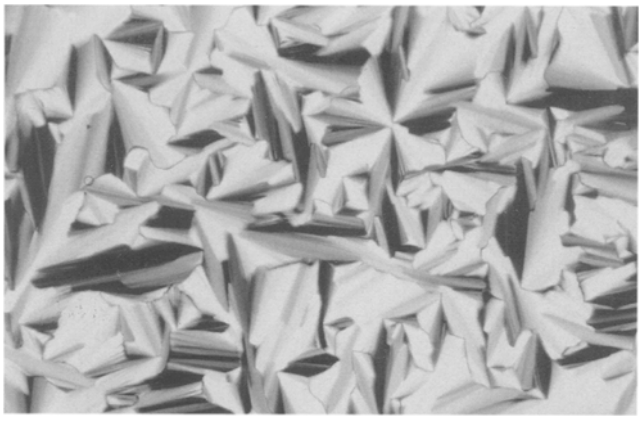

Fig. 7 Fan texture of the partially polymerised ω-UTAB hexagonal phase (crossed polarising filters, magnification 240). The cylinders lie parallel to the glass slide and the brushes correspond to line disclinations of strength $s = +1/2$, where the splaying out indicates variations in the curvature of groups of cylinders about the line disclination. The brushes lie at an angle of 5° to 10° to the polariser and analyser. Edge dislocations between individual fans are indicated by sharp dark lines, (67.7 wt% ω-UTAB sample at 25 °C)

isotropic fluid before the transition is complete at ~85 °C. Hence, the stability of the phase has not been significantly increased nor decreased due to the presence of polymer.

Although the optical microscopy results indicate that the polymer has been incorporated into the monomeric surfactant matrix it was necessary to determine if the polymer had been fully incorporated into this matrix without disturbing the surfactant molecules. This would then be in contrast with the case of ADAB where the polymer although having become an integral part of the liquid crystalline phase has not been formed by the retention of the monomeric surfactant geometry [1]. Hence, SAXS experiments were performed on the partially polymerised samples.

Diffraction patterns obtained at small- and wide-angles for samples in the concentrated micellar region consisted of one diffuse ring only. Comparison with the diffraction pattern for a monomeric sample (Table 1) indicates that the average distance between the aggregates in the partially and non-polymerised systems is very similar, which suggests that the nature of the micellar solution is largely undisturbed by the presence of polymer.

Likewise the partially polymerised hexagonal phase produced a diffraction pattern at small-angles comprised of three sharp Bragg peaks in the ratios of 1: $\sqrt{3}$: $\sqrt{4}$. No other peaks were detected, giving evidence that the underlying monomeric surfactant geometry is indeed maintained upon polymerisation. The chains were found to be in a fluid-like state by the presence of one diffuse ring at wide-angles.

Table 4 gives the structural parameters calculated assuming that the composition remains unchanged upon polymerisation (i.e., the phase is retained and no phase separation or transition has occurred). The specific volume of the surfactant is also assumed to vary little upon polymerisation. All equations were calculated for $T = 27$ °C. Comparison with the structural parameters determined for the monomeric hexagonal phase shows that using these assumptions the head group area, unit cell length and surfactant length are practically unchanged upon polymerisation (compare with Table 1). Hence, the original liquid crystalline phase geometry is undisturbed upon partial polymerisation with the original stability of the phase also being maintained.

Discussion

The position of the allyl polymerisable moiety has been shown to be crucial in determining the self-assembling properties of the surfactant and the extent to which polymerisation occurs either in an isotropic state or self-assembled form.

By comparing the concentration at which aggregation is initiated, the extent of dissociation of the bromide counterion, the excess surfactant concentration at the interface and the area per polar head group for ω-UTAB

Table 4 Structural parameters for the partially polymerised surfactant mesophases of ω-UTAB at $T = 27\,^{\circ}C$

ω-UTAB % (w/w)	Phase	Observed Q ($\AA^{-1}$)	Unit cell length (a) ($\AA$)	Volume fraction Φ	Surfactant aggregate thickness (d_s) ($\AA$)	Water thickness (d_w) ($\AA$)	Mean area per polar head (A) ($\AA^2$)	hkl
40.8	L_1	0.175	–	0.39	–	–	–	–
67.7	H_α	0.203	35.7	0.66	30.5	5.2	57.6	$10\bar{1}0$
		0.352						$11\bar{2}0$
		0.405						$20\bar{2}0$

(cmc $= 5.5 \pm 0.2 \times 10^{-2}$ M, $\beta = 33\%$, $A = 47 \pm 1$ $\AA^2$, $\Gamma_2^1 = 3.5 \pm 0.1 \times 10^{-3}$ mol·cm^{-2}), ADAB (cmc $= 1.1 \pm 0.1 \times 10^{-2}$ M, $\beta = 27\%$, $A = 58 \pm 1$ $\AA^2$, $\Gamma_2^1 = 2.9 \pm 0.1 \times 10^{-3}$ mol·cm^{-2}) [1] and DTAB (cmc $= 1.5 \pm 0.1 \times 10^{-2}$ M, $\beta = 34\%$, $A = 49 \pm 1$ $\AA^2$, $\Gamma_2^1 = 3.4 \pm 0.1 \times 10^{-3}$ mol·cm^{-2}) [7] an indication of the effect that incorporation of the allyl polymerisable group into the tail of the paraffinic chain can be obtained. The measured cmc for ω-UTAB, ADAB and DTAB indicates that by reducing the difference between the hydrophobic and hydrophillic regions of the surfactant the concentration at which surfactant aggregation is initiated is shifted to higher values. For all other measured parameters in the dilute concentration regime (i.e., close to the cmc) ω-UTAB closely mirrors DTAB as is expected since the two surfactants have the same head group. Whereas the solution behaviour of ADAB is significantly effected by the presence of the allyl moiety in its head group.

These results are carried over into the concentrated region of the phase diagram, where the phase progression of ω-UTAB with increasing surfactant concentration resembles that of DTAB [7]. Therefore, the presence of the carbon-carbon double bond at the end of the hydrocarbon chain does not significantly alter the balance of interactions between the surfactant molecules. The differences which do arise (i.e., decreased solubility at high surfactant concentrations and reduced phase stability) may be explained by an increase in the rigidity and an effective decrease in the length of the hydrocarbon chain. That is, by incorporating a carbon-carbon double bond into the tail of a hydrocarbon chain a subsequent restriction in the freedom of the paraffinic tail as compared with unsaturated hydrocarbon chains is introduced. This restriction in freedom promotes chain ordering which increases the temperature at which the order/disorder transition occurs, thereby shifting the Krafft curve to higher temperatures. Note that this is the reverse to what is observed for saturated and unsaturated surfactants when the unsaturation is confined to the beginning or middle of the hydrocarbon chain [42].

The decrease in stability of the liquid crystalline phases formed by ω-UTAB in comparison to DTAB may also be explained by the presence of the carbon-carbon double bond where the effective chain length is now approximately equivalent to a C_{10} hydrocarbon chain. Reduction in the chain length has been shown to affect both the type of liquid crystalline phases formed and also their stability with changes in temperature and composition. In general the stability of the phases is decreased as the effective hydrocarbon chain length is decreased. Hence, the presence of a carbon–carbon double bond at the end of the hydrocarbon chain in a quaternary ammonium surfactant reduces the temperature and compositional ranges over which the liquid crystalline phases are formed.

By polymerising the monomeric surfactant prior to aggregation it has been shown earlier that this reduced stability may be reversed. By covalently bonding the paraffinic tails forming low molecular polymers (which still have high degrees of freedom due to their low molecular weights and therefore lack of entanglement), the number of degrees of freedom of the surfactant have been increased sufficiently to allow both the cubic and lamellar phases to be stable at significantly reduced temperatures. Hence, the higher surfactant composition liquid crystalline phases have been stabilised by the polymerisation prior to self-assembly and the two phases are now accessible at room temperature.

Placement of the polymerisable group at the end of the hydrocarbon chain increases the probability that polymerisation will occur to a high yield but decreases the accessibility of the liquid crystalline phase by reducing their overall stability.

Polymerisation of the lower concentration ω-UTAB mesophases indicates that the integrity of the mesophase is not altered upon partial polymerisation. It must be noted though that it is unlikely that polymerisation of these phases has involved intra-aggregate polymerisation alone. In the case of polymerisation in micellar solutions the rate of micellar dissolution is much faster than the rate of polymerisation. Therefore at low concentrations the

micelles will have broken up before polymerisation of the aggregate is feasible. While this rate will decrease with increasing surfactant concentration the average length of a polymer chain is not altered (all polymer chains are comprised of a maximum of approximately 30 monomer units, as determined from dialysis) whereas, the average aggregation number of the surfactant aggregates increases with increasing concentration. Hence, the mechanism for polymerisation must involve growth of the polymer chains within a surfactant aggregate, in free solution or in a subsidiary aggregate differing from that in which it originated. That is, the polymer chains must either terminate within the original aggregate and then diffuse as a single entity moving freely within the aggregate and into and out of aggregates or a growing polymer chain, which is lost from its original aggregate, continues to grow and then terminates outside of the aggregates or becomes incorporated into another aggregate where it is finally terminated [43, 44]. Note that, either a growing or dead polymer chain may also act as seeds for the formation of a new aggregate.

Hence, the mechanism for polymerisation is very complex, but from this it can be ascertained that two things are crucial for intra-aggregate polymerisation only to occur. The rate of polymerisation must be shorter than the lifetime of the aggregates and the molecular weight of the growing polymer chain must be able to be controlled such that it is neither too low nor too high. That is, if the growing polymer chain continues to grow such that its molecular weight is greater than that of the aggregate it will begin to consume additional aggregates prior to termination, therefore destroying the phase. But if it is smaller than the molecular weight of the aggregate the surfactant aggregates will not be rigidified. Unfortunately, molecular weight is extremely difficult to control and in general polymerisable moieties with fast reaction rates form polymers with high molecular weights and those with slow reaction rates form polymer chains having low molecular weights.

A further problem was encountered during the polymerisation of a terminal paraffinic chain allyl group, the extent of polymerisation was reduced substantially upon surfactant self-assembly. Whereas, when the polymerisable group was contained within the head group the extent of polymerisation was equivalent in both self-assembled and non-self-assembled forms. The reduced extent of polymerisation is due therefore, to the mobility of the paraffinic tails. Such that unlike in the case of polymerisation in the head groups, where the head groups are confined to the surface of the aggregates and therefore ideally oriented for polymerisation [1], the paraffinic tails are generally uniformly distributed throughout the surfactant aggregate being found at the core, at the interface and at all allowed positions in between [45–55]. Therefore, once a free radical is formed it may not be able to find a second polymerisable group or suitably abstractable proton which are oriented appropriately before it is lost. That is, the surfactant aggregate acts as a cage inhibiting polymerisation. If a polymer chain is initiated it too may not be able to find an appropriately oriented carbon-carbon double bond and will be terminated by another growing chain or a free radical initiator or lost via diffusion from the aggregate or the original carbon-carbon double bond will be reformed.

Therefore, due to the lack of order of the hydrocarbon core of the surfactant aggregates and the confinement within the core for a time greater than that required for recombination of the free radicals the extent of polymerisation is reduced. The disruption to the interactions between the surfactant molecules and therefore the surfactant geometry is markedly reduced from that when polymerisation occurs in the head group region and as such the original average surfactant orientation is maintained upon polymerisation.

Conclusion

Placement of an allyl polymerisable group at the end of the hydrocarbon chain of a quaternary ammonium surfactant introduces an increased rigidity into the paraffinic chains reducing both the solubility of the surfactant at high concentrations and stability of the liquid crystalline phases formed.

Polymerisation in this position is facilitated in comparison to when the polymerisable moiety is contained within the head group region of the surfactant [1]. This is primarily due to the isolation of the allyl group from the region where the interactions between the surfactant molecules is concentrated with formation of the polymer not disrupting significantly these interactions which control the surfactant's self-assembly. Because of this the polymerised form of ω-UTAB self-assembles such that the liquid crystalline phases formed have an increased stability towards changes in temperature.

Polymerisation of the mesophases formed by this surfactant with water is such that the original underlying surfactant geometry is maintained. The extent of polymerisation in the surfactant's self-assembled form is reduced in comparison to polymerisation in an isotropic solution due to the surfactant aggregates acting as a cage inhibiting polymerisation.

Acknowledgments The surface tension measurements were performed by Nicole Moriarty and I also thank Calum Drummond and Patrick Kékicheff for some useful discussions. KMM was recipient of an Australian Postgraduate Research Award.

References

1. McGrath K, Drummond C (1995) ibid
2. Luzzati V, Reiss-Husson F (1966) Nature 210:1351–1352
3. Luzzati V, Tardieu A, Gulik-Krzywicki T, Rivas E, Reiss-Husson F (1968) Nature 220:485–488
4. Blackmore E, Tiddy G (1988) J Chem Soc, Faraday Trans 2 84:1115–1127
5. Fontell K (1990) Colloid Polym Sci 268:264–285
6. McGrath K (1994) Polymerisation of Surfactant Lyotropic Liquid Crystalline Phases. Thesis The Australian National University
7. McGrath K (1995) Langmuir 11: 1835–1839
8. Sprague E, Duecker D, Larrabee Jr C (1983) J Colloid Interface Sci 92: 416–421
9. Kamijo T, Harada H, Iizuka K (1983) Chem Pharm Bull 31:4189–4192
10. Simister E, Thomas R, Penfold J, Aveyard R, Binks B, Cooper P, Fletcher P, Lu J, Sokolowski A (1992) J Phys Chem 96:1383–1388
11. Lu J, Simister E, Thomas R, Penfold J (1993) J Phys Chem 97:6024–6033
12. Hutchinson E (1954) J Colloid Sci 9:191–196
13. Evans H (1956) J Chem Soc 579–586
14. Kamrath R, Franses E (1984) J Phys Chem 88:1642–1648
15. Tabor D, Underwood A (1989) J Chromatography 463:73–80
16. Rosevear F (1954) J Am Oil Chem Soc 31:628–639
17. Rosevear F (1968) J Soc Cosmetic Chemists 19:581–594
18. Oswald P, Kléman M (1981) J Phys France 42:1461–1472
19. Levelut A (1983) J Chim Phys 80: 149–161
20. Kléman M, Colliex C, Veyssié M (1976) In: Friberg S (ed) Lyotropic Liquid Crystals and the Structure of Biomembranes. American Chemical Society, Washington, DC, pp 71–84
21. Allain M, Kléman M (1987) J Phys France 48:1799–1807
22. Boltenhagen P, Lavrentovich O, Kléman M (1991) J Phys II France 1: 1233–1252
23. Luzzati V (1968) In: Chapman D (ed) Biological Membranes: Physical Fact and Function. Academic Press, London, pp 71–123
24. Luzzati V, Spegt P (1967) Nature 215:701–704
25. Fontell K (1981) Mol Cryst Liq Cryst 63:59–82
26. Rançon Y, Charvolin J (1987) J Phys France 48:1067–1073
27. Clerc M, Dubois-Violette E (1994) J Phys II France 4:275–286
28. Schwarz H (1890) Gesammelte Mathematische Abhandungen. Springer, Berlin
29. Schoen A (1970) Infinite Periodic Minimal Surfaces without Self-Intersections
30. Larsson K (1986) J Colloid Interface Sci 113:299–300
31. Andersson S, Hyde S, Larsson K, Lidin S (1988) Chem Rev 88:221–242
32. Hyde S (1989) J Phys Chem 93:1458–1464
33. Hyde S (1990) Progr Colloid Polym Sci 82:236–242
34. Luzzati V, Mustacchi H, Skoulios A, Husson F (1960) Acta Cryst 13:660–667
35. Husson F, Mustacchi H, Luzzati V (1960) Acta Cryst 13:668–677
36. Reiss-Husson F, Luzzati V (1964) J Phys Chem 68:3504–3510
37. Tardieu A, Luzzati V, Reman F (1973) J Mol Biol 75:711–733
38. Büldt G, Gally H, Seelig A, Seelig J, Zacci G (1978) Nature 271:182–184
39. Dilger J, Fisher L, Haydon D (1982) Chem Phys Lipids 30:159–176
40. Cabane B, Duplessix R, Zemb T (1985) J Phys France 46:2161–2178
41. Kékicheff P (1987) Des cylindres aux bicouches: étude structurale des transformations de phase dans un cristal liquide lyotrope. Thesis Thèse d'Etat, Université de Paris-Sud, Centre d'Orsay
42. Small D (1986) The Physical Chemistry of Lipids: From Alkanes to Phospholipids. Handbook of Lipid Research. Plenum Press, New York
43. Cochin D, Candau F, Zana R (1993) Macromolecules 26:5755–5764
44. Cochin D, Zana R, Candau F (1993) Macromolecules 26:5765–5771
45. Levine Y, Wilkins M (1971) Nature New Biology 230:69–76
46. Seelig J (1971) J Am Chem Soc 93: 5017–5022
47. de Gennes P (1974) Phys Lett 47A: 123–124
48. Marcelja S (1974) Biochim Biophys Acta 367:165–176
49. Zaccai G, Blasie J, Schoenborn B (1975) Proc Nat Acad Sci USA 72:376–380
50. Cabane B (1981) J Phys France 42:847–859
51. Gruen D (1981) J Colloid Interface Sci 84:281–283
52. Cabane B, Zemb T (1985) Nature 314:385
53. Gruen D (1985) J Phys Chem 89:146–153
54. Gruen D (1985) Progr Colloid Polymer Sci 70:6–16
55. Ennis J (1992) J Chem Phys 97:663–678